THE AMERICAN SOCIETY OF MECHANICAL ENGINEERS
Three Park Avenue, New York, N.Y. 10016-5990

.99-GT-358

3D Modelling of NOx Emissions from an Aircraft Afterburner

T J Foster and C W Wilson
Combustion and Emissions Section, Propulsion Department, DERA, DERA Pyestock, Farnborough, United Kingdom, GU14 0LS.

M Pourkashanian and A Williams,
Department of Fuel and Energy, University of Leeds, Leeds, United Kingdom, LS2 9JT.

Abstract

Aircraft fitted with afterburner systems for increased thrust have been observed to have NOx emissions with a higher proportion of nitrogen dioxide (NO_2) than non-augmented aircraft. These emissions are generally characterised by a brown plume and has implications for aircraft visibility and stealth as well as environmental considerations. This paper describes the CFD modelling of NOx emissions from a modern afterburner system with particular emphasis on the formation of nitric oxide (NO) and the subsequent conversion of NO to NO_2.

A commercial CFD code, was used to solve a three dimensional model of a "burn then mix" afterburner system under investigation. A post processor package has been developed and was used to calculate both NO and NO_2 concentrations. Four reheat settings were investigated; minimum, 25%, 50% and maximum reheat. For all conditions investigated the bulk of NOx emission was found in the core, stemming from the vitiated combustor air flow. NOx was also formed in the bypass stream, the production zone was found to be close to the fuel sprayers and flame stabiliser at minimum reheat, but moved downstream towards the exit nozzle as reheat power was increased. The model showed that for all the conditions under investigation, over 90% of the NOx produced in the reheat system was formed via the thermal-NO route.

The model has been compared with centre-line traverse data measured at the exit nozzle of the engine on a sea level static test bed. The predicted NOx emissions agreed quantitatively with the experimental measurements to within ± 5%.

Introduction

The requirement of a modern gas turbine aero-engine is for reduced emissions of pollutants to meet both civil legislation and military aircraft plume invisibility needs. Recent advances in gas turbine combustor technology have lead to a progressive reduction in the emissions of black carboneaous smoke from aircraft engines. However, these improvements; increased efficiency and consequently higher combustion temperatures, have lead to increased combustor exit emissions of nitrogen oxides (NOx), mainly in the form of nitric oxide (NO). If conditions are favourable NO can be rapidly converted to nitrogen dioxide (NO_2) in the engine jet pipe and near-field plume, giving rise to a yellow/brown plume. It has been observed that rapid conversion of NO to NO_2 can occur especially in reheat systems operating at low power where the average gas temperature and the presence of large concentrations of unburnt hydrocarbons favour NO_2 production.

In order to quantify and understand the effect of operating cycle on aircraft emissions measurements need to be made. A number of authors have made emissions measurements form aero-engines in flight (Fahey *et al.* 1995, Schulte and Schlager, 1996), although these measurements are expensive to make and give little information on the emissions at the exit plane of the engine. In order to understand these near-field plume effects measurements need to be made from engines installed on test beds. Such measurements have been made on military engines by a number of authors (Seto and Lyon, 1994, Foster and Wilson, 1997, Brundish *et al.*, 1997), all of which reported that high NO to NO_2 in the near-field plume of the engine under investigation especially at low reheat power levels.

Experimental measurements highlight the problem of nitrogen dioxide formation in the near-field plume and to understand the exact conditions leading to NO_2 formation computer modelling can be utilised. Generally computer models fall into two categories. The first is the detailed kinetic modelling approach, where a detailed understanding of the aerodynamics is sacrificed for a better knowledge of the reaction chemistry occurring (Foster and Wilson, 1997). The second is to use a Computational Fluid Dynamics (CFD) code to accurately predict the flow-field and through simplified reaction schemes, predict the temperature and emissions. CFD calculations have been used to aid understanding and to identify problems in a number of industrial applications such as power stations (Amin *et al.*, 1996) and furnaces (Al-Fawaz *et al.*, 1994).

Presented at the International Gas Turbine & Aeroengine Congress & Exhibition
Indianapolis, Indiana — June 7–June 10, 1999

In this paper we have taken experimental measurements from the exit plane of a reheated gas turbine engine and compared them to a CFD model at a number of power settings. The CFD model was also used to highlight regions of NO formation within the afterburner system with respect to potential NO to NO_2 conversion in the jet pipe and near-field plume.

NOx FORMATION

NO_x is the collective name given to the oxides of nitrogen; these being Nitric Oxide (NO), Nitrogen Dioxide (NO_2) and Nitrous Oxide (N_2O). In general NO_x is emitted from fossil fuel combustion in the form of NO, where upon it is oxidised to NO_2 in the atmosphere, although certain conditions can favour the production of NO_2 and N_2O leading to significant emissions (Miller and Bowman, 1989).

Thermal NO

The formation of thermal NO is determined by highly temperature dependent chemical reactions known as the extended Zeldovich mechanism.

The rate constant for these reactions have been measured in numerous experimental studies (Flower *et al.*, 1975, Blauwens *et al.*, 1977, Monat *et al.*, 1979) and the data obtained from these studies has been critically evaluated by Baulch *et al.* (1973) and Hanson and Salimian (1984). The expressions for the rate coefficients for extended Zeldovich reactions used in the current thermal NOx model are based on Hanson and Salimian (1984), and therefore the net rate of formation of is given by;

$$\frac{d[NO]_T}{dt} = k_1[O][N_2] + k_2[N][O_2] + k_3[N][OH] - k_{-1}[N][NO] - k_{-2}[O][NO] - k_{-3}[H][NO] \quad (1)$$

In order to calculate the formation rates of NO and N, the concentrations of O, H, and OH are required. The rate of formation of NO is significant only at high temperatures, greater than 1800K.

Prompt-NO

In flames where successful NO abatement measures have been used, often the total NO emissions can be dominated by prompt NO (Fenimore, 1971). Furthermore, there is substantial evidence that prompt NO can be formed in significant quantities in some combustion environments such as in the low-temperature, fuel-rich zones found in staged burners and gas turbines. Prompt NO is more predominant in rich flames and the actual formation involves a complex series of reactions and many possible intermediate species. A number of species, which result from fuel fragmentation, have been suggested as a main source of prompt NO in hydrocarbon flames, i.e., CH, CH_2, C, C_2H, etc. Recent studies (Schefer *et al.*, 1991) have shown that comparison of probability density distribution for the location of the peak NO with those obtained for the peak CH shows a close correspondence. This suggests that the majority of the NO at the flame base is prompt NO and in addition it can be concluded that the prediction of prompt NO formation within the flame requires coupling of the NO kinetics to the hydrocarbon combustion mechanism. Hydrocarbon combustion mechanisms involve a large number of steps, which can become very complex to solve and have a catastrophic effect on computer-processing time. In the present NO model, a global kinetic parameter derived by DeSoete (1975) and modified by Missaghi *et al.*, (1991) was used.

The De-Soete model was modified by using available experimental data from Bachmeier *et al.* (1973) and the effects of fuel type, (i.e. the number of carbon atoms) and air-fuel ratio were incorporated in a correction factor (f) applicable for aliphatic hydrocarbon fuels (Missaghi et al, 1991) and hence;

$$\frac{d[NO]_p}{dt} = f k_p [O_2]^a [N_2] [Fuel] \exp^{\left(\frac{-E_A}{RT}\right)} \quad s^{-1} \quad (2)$$

Where

$$f = 4.75 + C_1 n - C_2\phi + C_3\phi^2 - C_4\phi^3 \quad (3)$$

C_1 to C_4 are constants, n is the number of carbon atoms of hydrocarbon fuel and ϕ is the equivalence ratio. In the model the values for C_1 to C_4 were 8.19×10^{-2}, 23.2, 32 and 12.2 respectively. In order to obtain a realistic prediction of prompt NO, the oxygen reaction order should be calculated from composition data.

NO-Reburn and Fuel-NO

The reburn process at gas temperature range of 1600-2150K was obtained using a global approximation of :

$$\frac{d[NO]_{Re}}{dt} = -k_a[CH][NO] - K_b[CH_2][NO] - k_c[CH_3][NO] \quad (4)$$

Where the rates for k_a. k_b and k_c were obtained from Miller and Bowman, (1989) and $[CH_i]$ is calculated from partial equilibrium approximation.

Aviation kerosene contains little fuel bound nitrogen, therefore the Fuel-NO is not considered here and although additional NO can be formed by the nitrous oxide route it is only an important contributor to the total NO at lower temperature regimes than the work presented here.(Miller and Bowman, 1989, Michaud *et al.*, 1992, Johnsson *et al.*, 1992).

Nitrogen Dioxide

As emission regulations become more stringent there is an increasing interest in the formation of NO_2 in combustion products where it is in higher concentration than if slowly formed from NO in the atmosphere. The aircraft reheat systems and their application to civil (e.g. Concorde) and military engines where visible NO_2 is undesirable for various reasons

Nitrogen dioxide is formed by the reversible reactions of NO with HO_2, OH, O and O_2 via;

$$NO + HO_2 = NO_2 + OH \quad (5)$$

$$NO + OH = NO_2 + H \quad (6)$$

$$NO + O_2 = NO_2 + O \quad (7)$$

$$NO + O + M = NO_2 + M \quad (8)$$

At high temperatures, found in the flame zone, NO_2 is rapidly converted back to NO. However NO_2 conversion is favoured in the lower temperature regions where the combustion products have been rapidly cooled and high concentrations of the radical HO_2 can occur. Such conditions can be found in gas turbine engines where bleed

flows cool the combustor exhaust gases before entering the turbine stages and in afterburner systems (Seto and Lyon, 1994), and also in probe sampling from fuel lean combustion products (Bromly *et al.*, 1988). Under these low temperature conditions the reaction of HO_2 with other species is generally slow, with the exception of NO, reaction (5), and itself. The conversion of NO to NO_2 is enhanced strongly by the presence of any unburnt hydrocarbons (Hori *et al.*, 1992)

CFD Modelling Technique

In this study, CFD is demonstrated as an engineering tool and a commercially available code was used to solve the reacting fluid-flow and a post-processing package was then linked to the output to obtain distributions of NO concentrations. This code uses a moment method approach to solve the transport equations in finite-volume form. Turbulence closure for the turbulent convective fluxes has been achieved with the k-ε model in standard form. The source terms are evaluated using the slower of either the laminar reaction rates or the mixing rates determined by the eddy-break-up model (Magnussen and Hjertager, 1977). The flow field solution is subsequently used to solve the transport equation for the NO species. In order to solve equation (4), the concentration of quasi-steady species N, stable species (O_2 and N_2 etc.) the concentration of O atoms as well as free radical OH are required. Following a suggestion by Zeldovich, the thermal-NO formation mechanism can be de-coupled from the main combustion process, by assuming equilibrium values for temperature, stable species, O atoms and OH radicals. However, an error may be involved by this approximation. At present there is no definitive conclusion on the effect of super equilibrium on NO formation rates in turbulent flames. Peters and Donnerhak (1981) suggest that super-equilibrium radicals can account for no more than a 25% increase in thermal NO while fluid dynamics can have a dominant effect on NO formation rates. Bilger and Beck (1975), however, suggest that in turbulent diffusion flames the effect of O atom overshoot on NO formation rate is very important. The effect of super equilibrium O atom concentrations on NO formation rates has been investigated (Missaghi *et al.*, 1990) during CH_4/air combustion and the results indicated that the levels of NO emissions can be under-predicated by as much as 28% in the flame zone by assuming equilibrium O atom concentrations.

In this study two different techniques were adopted for prediction of O atom and OH radical concentrations. Allowance for super-equilibrium concentration of radicals in and near the primary reaction zone were made by imposing the data given by Dixon-Lewis (1980) on O and OH concentrations in methane/air flames at different strain rates. The rate of strain of the flame is related to the turbulent intensity of the combustion process. In addition an improved approximation of the O atoms and OH radicals is derived from the concentration of the stable species by use of the partial equilibrium assumption for the fast-flame reactions.

The oxygen concentration can be obtained from;

$$[O] = K_a[O_2]\,[CO]/[CO_2] \qquad (9)$$

and the hydroxyl concentration from;

$$[OH] = K_b\left([O_2]\,[CO]\,[H_2O]/[CO_2]\right)^{1/2} \qquad (10)$$

The equations 9 & 10 are derived from the partial equilibrium model by introducing the recombination rate of molecules. It should be noted, however, that this approach could only be employed if the concentration of CO is predicted properly in the flow-field calculations.

NO-NO_2 Conversion Modeling:

The chemistry of formation of NO_2 in flames and exhausts from combustion processes is considerably well researched especially through chemical kinetic modeling studies (e.g., Miller & Bowman, Nishioka et al. and Amano & Hase). It is believed that in addition to reactions 5 & 8 following reactions may contribute towards NO-NO_2 conversion process:

$$NO + RO_2 \rightarrow NO_2 + RO \qquad (11)$$
$$NO + HORO_2 \rightarrow NO_2 + HORO \qquad (12)$$

Reaction flux calculations indicates that NO-NO_2 conversion process predominantly controlled through the reaction 4 under normal operating conditions. However kinetic studies have indicated that reactions 11 & 12 contribute less than 15% to NO-NO_2 conversion. Therefore for modeling purposes, it become of paramount importance to determine source of HO_2 production through following reaction steps:

$$[\text{Fuel Fragments Alkyl}] + O_2 \text{ Olefin} + HO_2 \qquad (13)$$
$$HCO + O_2 \rightarrow CO_2 + HO_2 \qquad (14)$$
$$HO_2 + H \rightarrow OH + OH \qquad (15)$$
$$HO_2 + O \rightarrow OH + O_2 \qquad (16)$$
$$HO_2 + OH \rightarrow H_2O + O_2 \qquad (17)$$
$$HO_2 + H \rightarrow H_2O + O \qquad (18)$$
$$H + O_2 + M \rightarrow HO_2 + M \qquad (19)$$

The NO_2 reduction takes place through reactions 6 & 7.

The production rate of NO_2 formation reaches a peak typically between 500 K and 700 K whereas that of NO_2 reduction occurs between 800 K and 1000 K. The low levels of NO found in un-cooled flames are the results of a delicate balance between the consecutive production and consumption rates of similar magnitudes. This delicate balance is upset as soon as cooling is imposed on the combustion products. This effect was studied in particular by Amano and Hase. In the case of two-stage cooling, the conversion was dependent not only on the cooling rate but also on the temperature of the plateau and on its duration. Increasing the initial NO concentration from 50 ppm was found to have very little effect on the previous conclusions, whereas below 30 ppm, the conversion increased exponentially regardless of cooling conditions as was also found by Hand et al. Kinetic studies like these have always been mitigated by lack of experimental corroboration, i.e. Amano and Hase only published experimental data corresponding to the low NO/NO_2 conversion conditions. This lack of experimental data is partly due to the difficulties in measuring NO_2 accurately. Indeed, conversion of NO to NO_2 in the sampling probe due to cooling has been researched but there is a lack in precise descriptions of the experimental conditions of sampling.

Therefore in-order to predict the NO_2 emission from a combustion device using a post-processor combined with commercial CFD code, a simple global approach was implemented. After careful

considerations of all the available models for predicting NO_2 formation in the combustion process, it was decided that a model based on partial equilibrium approach could be a useful engineering tool for calculating the NO_2 concentration. When applied to practical engineering problems, this technique requires significantly lower computational time than using detailed reaction mechanism. Assuming that HO_2 formation and destruction can be represented via reactions 13-19 and at high temperature the reactions rates of forward and backward reactions are so fast, that one obtains partial equilibrium for the reactions 13-18. However as shown above, the concentration of H, OH and O can be calculated from partial equilibrium assumption and therefore the HO_2 concentration can be calculated from reactions 14-19. The rate of formation and consumption of the HO_2 concentration is related to reaction intermediates through the fast exchange reactions 14-19. The use of partial equilibrium assumption greatly simplifies the analysis of otherwise very complex chemical kinetic routes. The reactions 13-18 is fast compared to three-body recombination reactions that ultimately eliminate the radicals from the system. To a first approximation, by considering that the reaction intermediates are at equilibrium with one another through reactions 14-19, the partial-equilibrium concentration of HO_2 may be expressed by the following equation:

$$[HO_2]_{pe}=A/B \qquad (20)$$

Where all the equilibrium constant are in concentration units and:

$$A= \{[H_2O][O_2]+[H_2O][O]+[O_2][OH]+[OH]^2\} \qquad (21a)$$
$$B= \{K_{32}[OH]+k_{33}[H]+K_{31}[O]+K_{30}[H]\} \qquad (21b)$$

It is important to mention that the accuracy of HO_2 concentration will depend significantly on accurate prediction of H concentration. An empirical approach (non-temperature dependent Arrheninus expression) was used to represent the global reaction 14.
Reactions 5-7 were used to calculate the net rate of production of NO_2. The reaction rate parameters (A, B, and E) was obtained from Hanson and Salimian.

Turbulence/Chemistry Interaction Model

To predict the NO scalar field, the conservation equation has been solved subsequently to solving the flow field. The source term ω_{NO} is evaluated using a PDF approach. Thermal NO formation depends critically on the mean O radical concentration with allowance for non-equilibrium radical concentrations. The prompt NO concentration field in turn depends critically on the CH radical concentration and temperature. Therefore, the turbulent model used in the present investigation is improved by using a two depended variable system for which the first moments are obtained from the solution of the transport equations. The mean turbulent reaction rate ω_{NO} can be described in terms of the instantaneous rate ω and a joint PDF of various variables;

$$\varpi = \int \omega(v_1 v_2 .....) p(v_1 v_2 .....) dv_1 dv_2 ..... \qquad (22)$$

Where v_1, v_2 ,... are temperature and species concentration and therefore for a two variable joint PDF;

$$\omega_{NO} = \int \omega_{NO}(v_1 v_2) p(v_1 v_2) dv_1 dv_2 \qquad (23)$$

Where ϖ_{NO} is the mean turbulent rate of production of NO, ω_{NO} is the instantaneous rate of production given by equations 1 and 4, and $p(v_1\ v_2)$ is the joint PDF of the variables v_1 and v_2. If it is further assumed that the variables v_1 and v_2 are statistically independent;

$$p(v_1 v_2) \neq p_1(v_1) p_2(v_2) \qquad (24)$$

Where p_1 and p_2 are assumed here to be two moment beta functions, the equation for the beta function is the second moment v_2 was assumed to be related to the first by;

$$v^2 = s(v(1-v)) \qquad (25)$$

Where s is a coefficient to be selected to represent the intensity of fluctuation and the term in the brackets is the top limit of the second moment. Higher values correspond to higher Dahmkohler numbers, representing wrinkled laminar flame regimes, while lower values represent distributed combustion regimes.

In order to limit the computational time, each beta function was evaluated at 10 points on a histogram basis. A sensitivity analysis prior to the detailed computation was carried out for the beta functions, so that when V_1 or V_2 were near their extreme values, the associated beta function was replaced by a delta function and the instantaneous rate of production was directly incorporated.

The code is written so that the variable V_1 and V_2 can be selected depending on the type of NO formation in question. For example, for thermal NO, V_1 was temperature and V_2 was O radical mass fraction while for prompt NO they were temperature and CH mean mass fraction, respectively. At each step during two interactions, the extreme limits of V_1 and V_2 were calculated and the integration in equation (23) was obtained over the whole range of V_1 and V_2 at the interaction step in question.

The boundary condition for CFD model in terms of gas composition was obtained from engine measurements at the max-dry engine operating condition. All these species were effectively the same concentration as that of the combustor exit to allow the dilution by turbine blade cooling. The air mass flow rate through the inlet slots and jet orifices were computed using a 1-D flow distribution code. The computational mesh comprises 80 x 45 x 65 nodes reflecting a compromise between geometrical fidelity and grid dependent solution.

Experimental Measurements

Combined temperature and emissions measurements were taken at the exit nozzle of a reheated gas turbine engine, fitted with a burn and mix reheat system, installed on a sea level static test bed at DERA Pyestock. The sampling probe was capable of traversing the engine diameter in both horizontal and vertical planes and was made stainless steel and is shown in Figure 1. High pressure hot water was used both to cool the probe and condition the gas sample. The sampling probe was connected to the analysers by ca. 15m of 6mm i.d. insulated stainless steel tubing, maintained at 150±15°C. A chemiluminescent analyser was used to measure NO and NOx. Carbon monoxide and dioxide were measured by NDIR analysers and total unburnt hydrocarbons were measured using a FID. Gas temperature was measured using a shielded platinum/platinum-

rhodium thermocouple, located 10mm above the gas-sampling orifice. Gas analysis was made in accordance with ARP specification. All the instruments were calibrated to take into account the interference from gases and it is believed that accuracy of measurements is within 2% of the reading.

During the test programme gas temperature and emissions measurements were made across the centre line of the exhaust nozzle with the engine at idle, maximum continuous and a number of reheat power settings.

Results and Discussion

NOx, NO and NO_2 emission measurements for the engine running at maximum continuous and reheat conditions are shown in Figures 2, 3 and 4 respectively. For all the results shown the emissions values have been non-dimensionalised by dividing the respective point measurement by the maximum NOx concentration measured during the whole experimental trial. The results in Figure 2 show that at low afterburner settings there is a net reduction in NOx emissions compared to the non reheated, maximum continuous, condition. This reduction is probably due to a reburning effect, as the temperature and poor reheat combustion efficiency, and consequently high unburnt hydrocarbon levels, would favour reburning of the NO formed in the combustor at these conditions. NOx destroying reactions within the probe was ruled out as a separate test was performed in order to investigate probe-induced reactions and no loss of NOx was observed. As power is further augmented NOx emissions increase reaching a maximum in the order of 200 ppmv. The NOx results at 50% and maximum reheat show two distinct emission peaks in the traverse corresponding to the location of the bypass sprayers and the method of fuelling the afterburner system. At these conditions the bypass stream is running close to stoichiometric combustion conditions and consequently forming NO via the thermal route, as highlighted in the experimental and NO measurements in Figure 3 and the CFD NOx predictions shown in Figures 8 and 9.

Figure 4 shows measured NO_2 concentrations at the engine exit plane. When compared to the NO results in Figure 3 it can be seen that at dry operation the NOx emission is predominantly NO, however, at low reheat power settings, NO_2 makes up a large proportion, approximately 80%, of the total NOx emission. Probe effects were again investigated and it was found that at these inefficient reheat conditions NO to NO_2 conversion is accelerated within the probe tip by the reaction with HO_2 radicals. The true proportion of NO_2 was approximately 30% of the total NOx at the centre point of the traverse although further conversion within the test house detuner gave rise to a visible brown/yellow plume at the detuner exit. At 50% reheat and above it can be seen that the nitrogen dioxide results in Figure 4 shows that NO_2 formation occurs mainly at the edge of the exhaust jet as relatively cold air, from jet pipe cooling and some entrained ambient air, interact with the hot combusting jet leading to conditions favouring NO_2 formation. This trend can also be seen at lower afterburner powers although it is somewhat swamped by probe effects.

In order to clarify the experimental observations a CFD model, based on a single sector of the reheat system, was used and is outlined in Figure 5. In this paper full CFD predictions are only shown for maximum reheat. Figures 6 and 7 show temperature predictions for the sector and full engine respectively, NOx predictions are shown in Figures 8 and 9. From the temperature predictions it can be seen that there is little mixing between the core and bypass streams within the jet pipe. The predicted temperature field shows a slight increase in the core gas temperature, reaching a maximum around 1600K, with the flame anchored by the gutters. Combustion in the bypass stream is initiated and stabilised by the fuel from colander, which in turn ignites the fuel from the bypass sprayers. A peak exit plane temperature of 2200K is predicted, although combustion will continue downstream of the exit plane. The results also show that the cooling air film is maintained down the length of the jet pipe.

From the NOx predictions it can be seen that the reheat system does not produce huge quantities of NOx. A small amount of NOx is formed in the core stream in the flames stabilised by the gutters, although at lower reheat powers some NOx formed in the combustor is destroyed in this region via the reverse of the reactions in the CFD code. At maximum reheat there is some NOx formed within the bypass stream, via the thermal-NO route, corresponding to the high temperature regions. However, very short residence times prohibit the formation of vast quantities of NO within the reheat system. A comparison of experimental and predicted NOx at a number of reheat settings is shown in Figure 10. It can be seen that the results compare favourably, both in absolute value and in the trends across the traverse. There is a slight discrepancy at minimum reheat as the CFD model under-predicts the combustion intensity, and consequently the temperature and NOx. But despite the complexity of the problem being modelled the influence of features, such as the bypass sprayers on the exit profile, are being successfully predicted.
Finally Fig 11 shows the comparison between the measured and predicted NO_2 concentration for two different reheat setting. Predicted results indicate that with decreasing reheat NO_2 emission is increased. However in the simulation the increase is less strong than measurements. The predicted and measured NO_2 emission gives the largest difference at the centre of the engine. Overall the numerical model under-predicts the NO-NO_2 conversion rate and consequently the NO_2 formation. This difference partly may be attributed to the partial equilibrium assumption that was used to predict HO_2 concentration. In order to evaluate the partial equilibrium assumption the description of formation and destruction of entire pool of intermediates during combustion process is needed. Another possible source of error could be the omission of following chemical reactions from the NO-NO_2 conversion mechanism used in this study:

$$CO + O_2 \rightarrow CO_2 + O \quad (26)$$
$$O + H_2O \rightarrow OH + OH \quad (27)$$
$$CO + OH \rightarrow CO_2 + H \quad (28)$$

Where the input from reactions 26 & 27 are needed to initiate the process followed by an input from reaction 28 which effect the H radical concentration in the system to initiate reaction 19 and simultaneously oxidising CO to CO_2. At present validation work is being carried out by following a weighted sum of the concentrations of the species in the radical pool.

Conclusions

The aim of this work was to make a series of experimental measurements in the exit plane of a reheated gas turbine engine and

compare them to predictions from a CFD model. The system to be modelled was complicated, involving high flow-rates, mutli-point fuel injection and vitiated air, but the results reported in this paper show good agreement between the two techniques both qualitatively and quantitatively. The CFD model showed where NOx is produced and, in the future, where NO to NO_2 conversion occurs within the reheat system allowing the development of smart fuelling systems that minimise the production of NO and prevent the formation of visible emissions. The work also highlights problems associated with probe induced reactions in making measurements of NO and NO_2 in fuel rich regions, such as those found at minimum reheat, and needs to be addressed to validate the CFD predictions.

References

Al-Fawaz, A. Dearden, L. M., Hedley, J. T., Pourkashanian, M., Williams, A. and Yap, L. NOx Formation in Geometrically Scaled Gas Fired Industrial Burners. *25th Symposium (International) on Combustion*. The Combustion Institute p. 1027. (1994).

Amano, T, and Hase, K. "Cooling Condition of Hot Exhaust Gas For Low Conversion of NO to NO_2". *Journal of the Institute of Energy*, December 1994, 67,pp 174-180, 1994.

Amin, E. M., Andrews, G. E., Pourkashanian, M., Williams, A. and Yetter, R. A. "Comparison Study of Pressure Effects on Pollutant Generation in Gas Turbine Combustors". Journal of Engineering for Gas Turbines and Power. 118. p 773. (1996).

Bachmeier, F., Eberius, K.H. and Just I. *Combustion Science and Technology*, Vol. 7. p. 77. (1973).

Baulch, D.L., Dysdale, D.D., Horne, D.G., and Lloyd, A.C., "Evaluated Kinetic Data For High Temperature Reaction", Vol. 1,2,3, Butterworth. (1973).

Bilger, R.W. and Beck, R.E., *15th Symposium (International) on Combustion*. The Combustion Institute. p. 541. (1975).

Blauwens, J., Smets, B., and Peeters, B. *16th Symposium (International) on Combustion*. The Combustion Institute. p. 1055. (1977).

Bromly, J. H., Barnes, F. J. and Little, L. H. "The Effects of Low Concentrations of CO, H_2 and Hydrocarbons on NO_2/NO Ratios in Heated Gases", *Journal of the Institute of Energy*. 61. pp. 89-97. (1988).

DeSoete, G. G. Overall Reaction Rates of NO and N_2 Formation From Fuel Nitrogen. *15th Symposium (International) on Combustion*, The Combustion Institute. pp. 1093-1102. (1975).

Dixon-Lewis, G. Fifth International Conference on Numerical Combustion, TECFLAM, 1993.

Fahey, D. W. et al. "In Situ Observations in Aircraft Exhaust Plumes in the Lower Stratosphere at Mid-latitudes", *Journal of Geophysical Research*. 100. pp. 3065-3074. (1995).

Fenimore, C.P. *13th Symposium (International) on Combustion*. The Combustion Institute. p. 373. (1971).

Flower, W.L. Hanson, R.K. and Kruger, C.H. *15th Symposium (International) on Combustion*. The Combustion Institute. p. 823. (1975).

Foster, T.J. and Wilson, C.W. Detailed Chemical Modelling Predictions of Emissions from a Reheated Gas Turbine Engine with Application to Future Subersonic Aircraft. ASME PAPER GT-97-(1997).

Hand, G., Missaghi, M., Pourkashanian, M. and Williams, A. "Experimental studies and computer modelling of nitrogen oxides in a cylindrical natural gas fired furnace", IFRF 9th Members Conference, May 1989.

Hanson, R.K., and Salimian, S. Survey of Rate Constants in H/N/O System. p. 361. Combustion Chemistry, (Ed. W.C. Gardiner). (1984).

Hori, H., Matsunaga, N., Malte, P. C. and Marinov, N. M. The Effect of Low Concentration Fuels on the Conversion of NO to NO_2. *24th Symposium (International) on Combustion*. The Combustion Institute. pp. 909-916. (1992).

Johnsson, J. E., Glarborg, P. and Dam-Johansen, K. "Thermal Dissociation of Nitrous Oxide at Medium Temperatures", *24th Symposium (International) on Combustion*. The Combustion Institute. pp. 917-923. (1992).

Magnussen, B.F. and Hjertager, B.H. *16th Symposium (International) on Combustion*. The Combustion Institute. p. 719. (1977).

Michaud, M. G., Westmoreland, P. R. and Feitelberg, A. S. Chemical Mechanisms of NOx Formation for Gas Turbine Conditions. *24th Symposium (International) on Combustion*. The Combustion Institute. pp. 879-889. (1992).

Miller, J. A. and Bowman, C. T. Mechanism and Modelling of Nitrogen Chemistry in Combustion. *Progress in Energy and Combustion Science*. 15. pp. 287-338. (1989).

Miller, J.A., Branch, M.C., McLean, W. J., Chandler, D.W., Smooke, M.D. and Kee, R. J., *20th Symposium (International) on Combustion*. The Combustion Institute. p. 673. (1985).

Missaghi, M., Pourkashanian, M., Williams, A. and Yap, L. Proceedings of American Flame Days Conference. USA. (1990).

Missaghi, M., Pourkashanian, M., Williams, A., Yap, L. Predictions of NOx Emissions from Oxygen-Enriched low NOx Burners. *Proceedings of the International Conference on Environmental Control of Combustion*. Honolulu, Hawaii, AFRC. (1991).

Monat, J.P., Hanson, R.K., and Kruger, C.H. *17th Symposium (International) on Combustian*. The Combustion Institute. p 543. (1979).

Hori, M. "Nitrogen Dioxide Formation by the Mixing of Hot Combustion Gas with Cold Air", *Twenty Second Sympasium (International) on Combustian*. The Combustion Institute, 1988.

Nishioka, M., Nakagawa, S., Ishikawa, Y. and Takeno, T. "NO Emission Characteristics of Methane-Air Double Flame". *Combustian and Flame* 98:127-138, 1994.

Peters, N. and Donnerhack. S. *18th Symposium (International) on Combustion*. The Combustion Institute. p. 33. (1981).

Schefer, R. W. Namazian, M. and Kelly, J. Combustion Research Facility News, Sandia National Laboratories. Vol 3., No. 4, (1991).

Schulte, P. and Schlager, H. In-flight measurements of cruise altitude nitric oxide emission indices of commercial jet aircraft. *Geophys. Res. Lett.* 23, pp. 165-168. (1996).

Seto, S. P. and Lyon, T. F. Nitrogen Oxide Emissions Characteristics of Augmented Turbofan Engines. *Journal of Engineering for Gas Turbines and Power*. 116. pp. 478-482. (1994).

Brundish, K. D, Moncriet, J., Wilson, C. W. and Wooton, A. DIAL Measurements on a Gas Turbine Exhaust. AGARD Fall Meeting (1997).

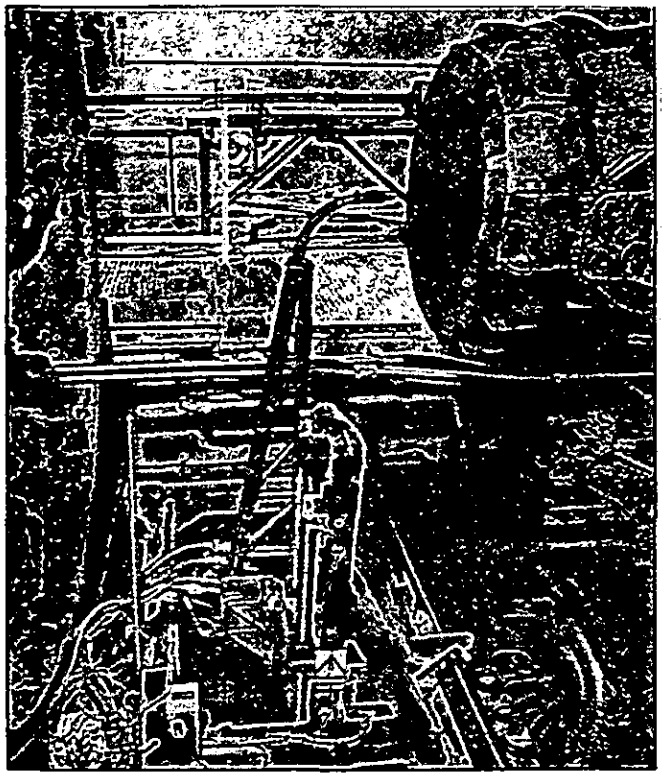

Figure 1. Photograph showing the traversing gas sampling probe insitu.

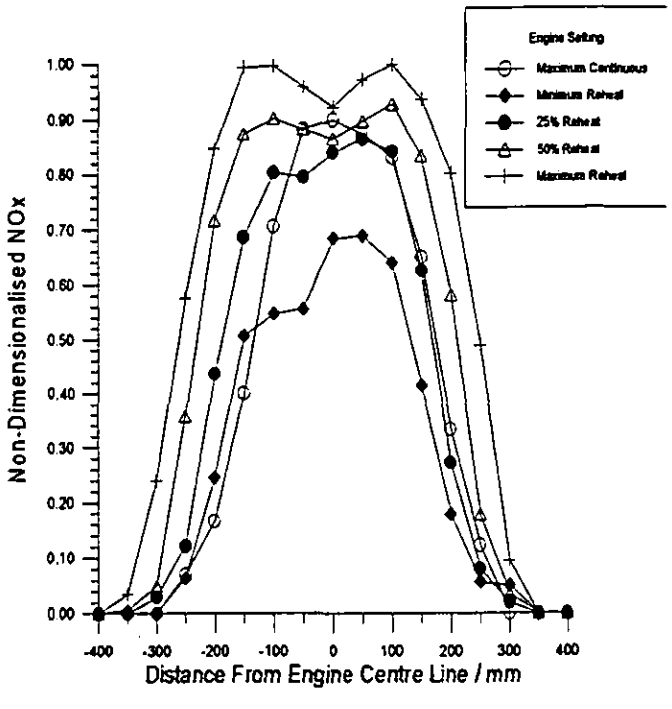

Figure 2. Engine exit centre line NOx measurements at maximum continuous and reheat conditions.

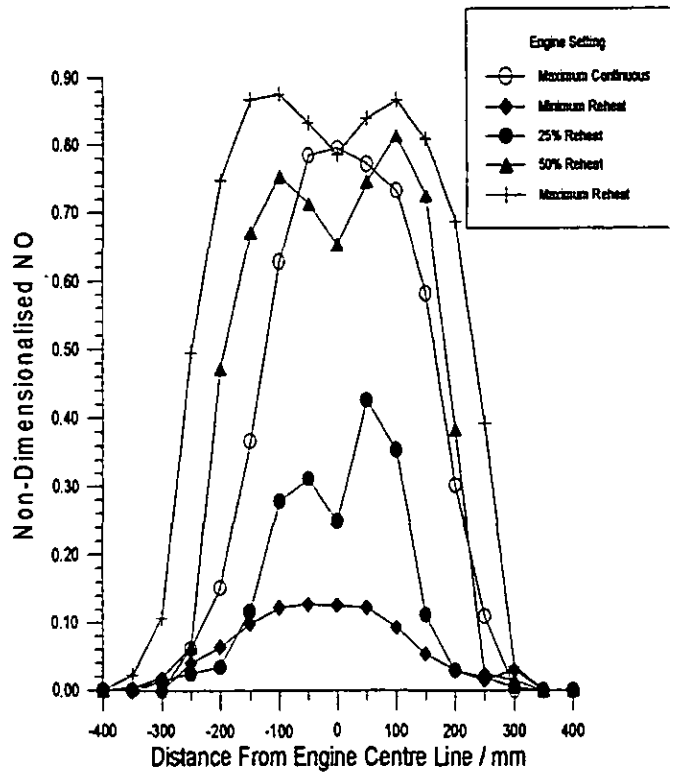

Figure 3. Engine exit centre line NO measurements at maximum continuous and reheat conditions.

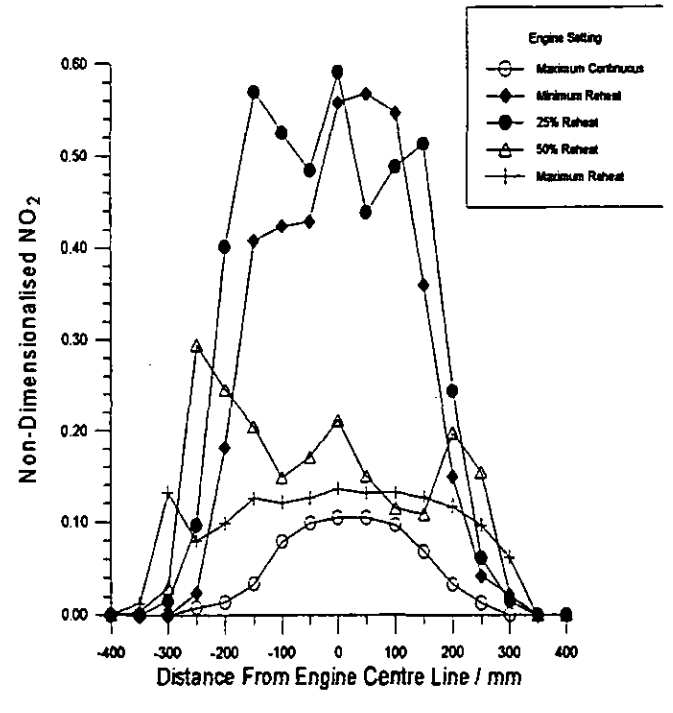

Figure 4. Engine exit centre line NO_2 measurements at maximum continuous and reheat conditions.

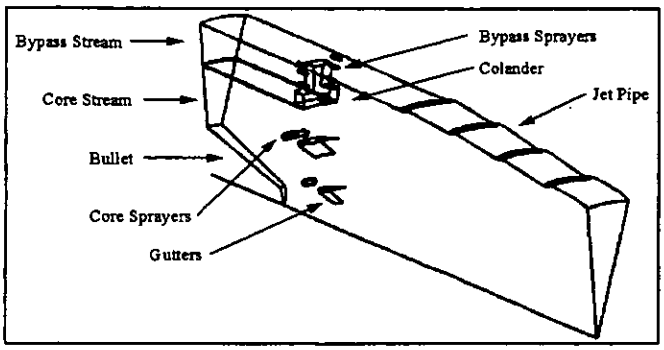

Figure 5. CFD model outline of the reheat section.

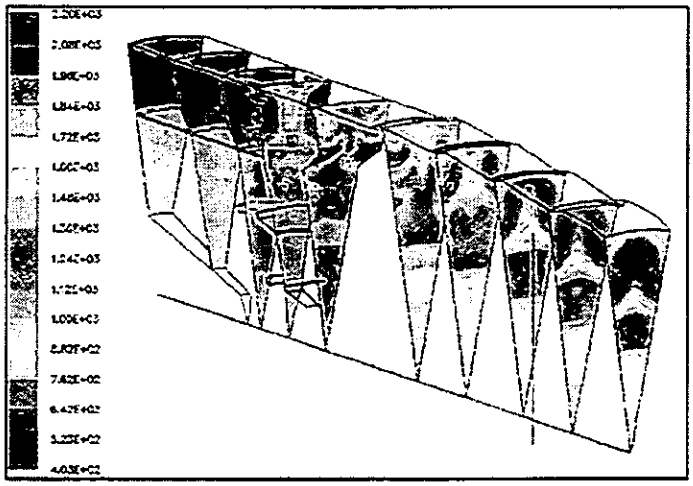

Figure 6. CFD Temperature prediction at various planes in the reheat section.

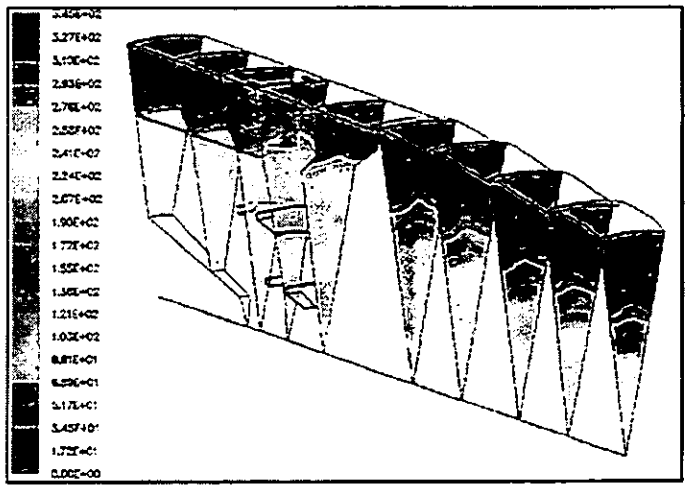

Figure 8. CFD NOx prediction at various planes in the reheat section.

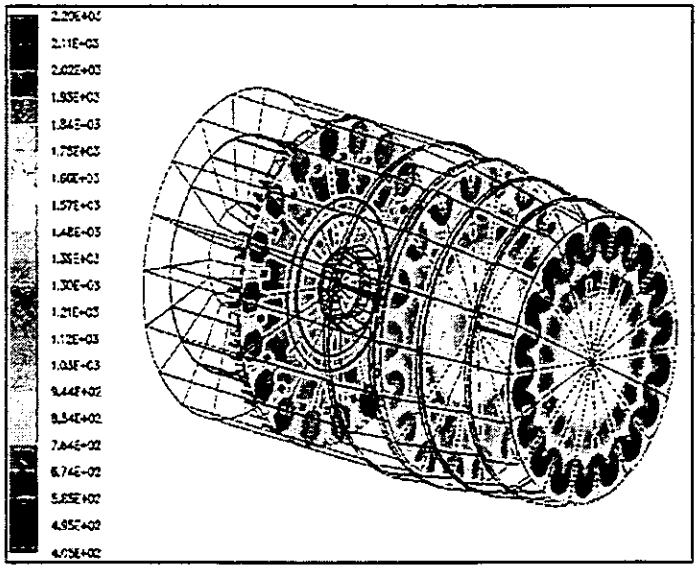

Figure 7. CFD Temperature prediction shown for the complete engine at various planes down the reheat system.

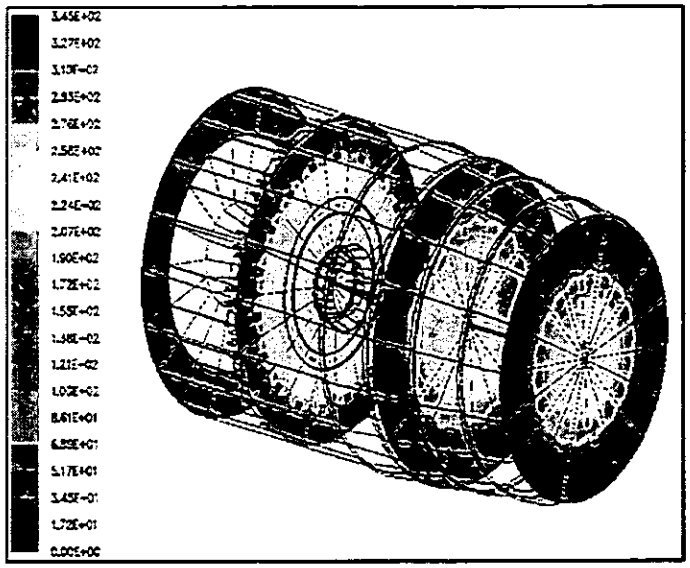

Figure 9. CFD NOx prediction shown for the complete engine at various planes down the reheat system

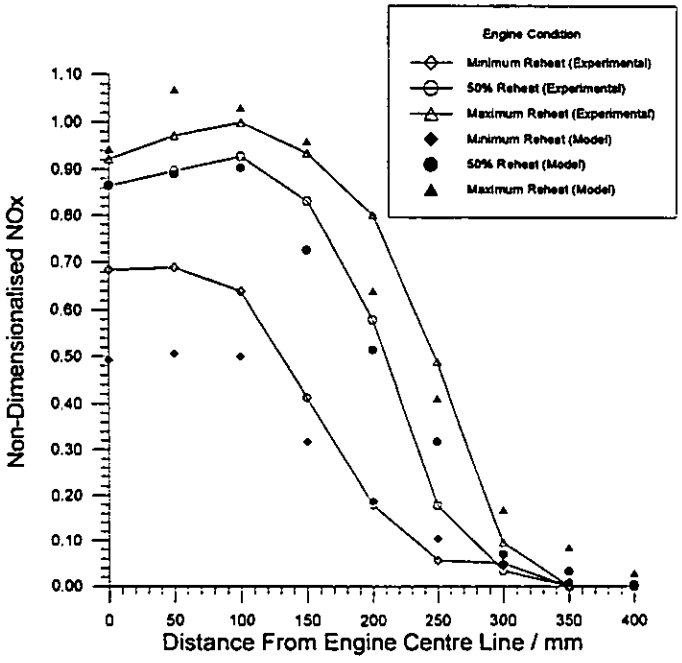

Figure 10. Comparison of NOx concentrations made by experimental measurement and CFD predictions

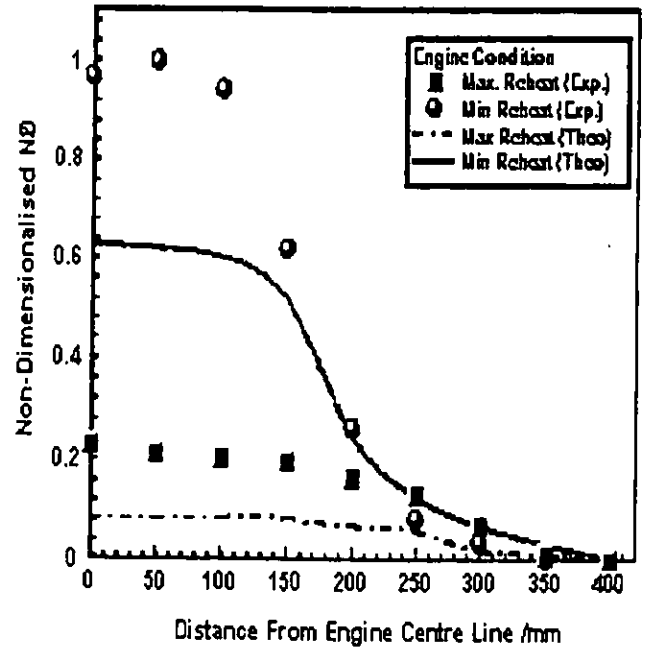

Figure 11. Comparison of NO_2 concentrations made by experimental measurement and CFD predictions at a # of condition